

Single-Occupancy Binding in Simple Bounded and Unbounded Systems

Mark F. Schumaker

Department of Mathematics, Washington State University, Pullman, WA 99164-3113, USA

Received: 14 August 2006 / Accepted: 9 February 2007 / Published online: 19 April 2007
© Society for Mathematical Biology 2007

Abstract The number of substrate molecules that can bind to the active site of an enzyme at one time is constrained. This paper develops boundary conditions that correspond to the constraint of single-occupancy binding. Two simple models of substrate molecules diffusing to a single-occupancy site are considered. In the interval model, a fixed number of substrate molecules diffuse in a bounded domain. In the spherical model, a varying number of molecules diffuse in a domain with boundary conditions that model contact with a reservoir containing a large number of substrate molecules. When the diffusive time scale is much shorter than the time scale for entering the single-occupancy site, the dynamics of binding are accurately described by simple approximations.

Keywords Single-occupancy binding · Random walk · Diffusion · Boundary conditions · Smoluchowski equation

1. Introduction

Single-occupancy binding is very common in biological systems. For example, when a substrate molecule binds to the active site of an enzyme, no other substrate may be able to bind to that active site until the first molecule dissociates, or until an enzymatic reaction takes place and the products dissociate. Computer simulation of substrate molecules binding to enzymes are an important component in an attempt to understand the mechanism of biological systems at the molecular level. Random walk simulation of the trajectories of a large number of substrate molecules diffusing in the vicinity of an active site is computationally intensive. Instead, it would be useful to be able to directly solve the partial differential equations that govern the time evolution of the probability densities (Song et al., 2004). This paper obtains boundary conditions for diffusive differential equations in two simple models of diffusion to a single-occupancy binding site.

The interval model is a model of diffusion in a bounded domain in which the number of substrate molecules is fixed. We consider diffusion in the interval $0 < x < 1$. Use of the simple diffusion equation implicitly assumes that the underlying particle trajectories are

noninteracting in the interior of the interval. However, there is a single-occupancy binding site at $x = 0$. The spherical model is a model of diffusion in an unbounded domain that contains a very large number of substrate molecules. The system is assumed to be spherically symmetrical and considers spatial variation as a function of the radial variable r . Particle trajectories in the domain $r > 1$ are assumed to be noninteracting, but there is a single-occupancy binding site at $r = 1$. When the diffusion equation is written in terms of r , a Smoluchowski equation is obtained which includes a geometrical drift term. These models are examples of exclusion processes (Liggett, 1985).

The interval and spherical models are constructed as the diffusion limits of random walks. Discrete-time random walks are used. This formulation has the advantage that, if site occupation probabilities are known at time t , it is very easy to determine these probabilities after a finite positive time step. On the other hand, numerical simulation of continuous-time random walks may be much more efficient when time scales are widely separated (Gillespie, 1977). For consistency, we use a discrete-time algorithm which is sufficient for the simulations described below.

A biological example of diffusion in a bounded domain is diffusion of substrate molecules between cytochrome b_6f and photosystem II in putative microdomains in the thylakoid membranes of chloroplasts of higher plants (see Kirchoff et al. (2000); their Fig. 10 is a cartoon of a proposed structure). A typical "small" domain would be a patch of area on the membrane, with a characteristic length of few tens of nanometers, surrounded by proteins which are immobile on the time scale of interest. It might include 1 or 2 photosystem II proteins, a cytochrome b_6f protein, and 5 to 10 plastoquinone molecules that are substrates for binding sites on the proteins. The large photosystem II proteins are dimers; each monomer subunit has a plastoquinone binding site. The smaller cytochrome b_6f proteins are also dimers; each monomer has two plastoquinone binding sites. An example of diffusion in an effectively unbounded domain is diffusion of ATP to the active site of the dynein ATPase in an homogeneous, macroscopic, experimental preparation (Omoto and Johnson, 1986).

2. The interval model

This section considers diffusion on a simple bounded domain, an interval, with a single-occupancy binding site at one endpoint. Begin by introducing dimensionless variables. Consider the diffusion equation on the interval $0 < X < L$:

$$\frac{\partial C}{\partial t'} = D \frac{\partial^2 C}{\partial X^2}. \quad (1)$$

Write (dimensions of X) = $[X]$, then $[X]$ = length, $[t']$ = time, $[C]$ = length⁻¹ and $[D]$ = length²/time. Introduce the dimensionless spatial coordinate $x = X/L$ and time $t = t'/t'_D$, where the diffusive time scale $t'_D = L^2/D$. Defining the dimensionless concentration $c(x, t) = LC(X, t')$, obtain the diffusion equation in dimensionless variables:

$$\frac{\partial c}{\partial t} = \frac{\partial^2 c}{\partial x^2}. \quad (2)$$

Fick's law states that the probability flux is proportional to the concentration gradient: $J = -D(\partial C/\partial X)$. Introduce the dimensionless flux $j = t'_D J$, to give

$$j = -\partial c/\partial x. \quad (3)$$

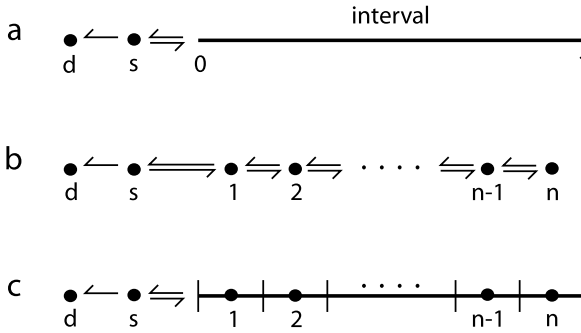


Fig. 1 (a) State diagram of the interval model. Diffusion takes place in the interval $0 < x < 1$. s is the single-occupancy binding site. The transition $s \rightarrow d$ signifies conversion of substrate to product, immediately followed by release of product. (b) Random walk n of the sequence whose limit is the interval model. (c) Random walk site i corresponds to the midpoint of subinterval i .

The diffusion equation on the interval $0 < x < 1$ with a single-occupancy boundary condition at $x = 0$ is obtained as the diffusion limit of a sequence of random walks. Fig. 1a shows the state diagram of the interval model. Diffusion takes place in the interval. A diffusing substrate can enter the binding site s and either escape from s back to the interval or enter the state d . This system of coupled diffusion and Markov jumps is obtained as the limit of the sequence whose n th random walk is shown in Fig. 1b. The interval model is obtained in the diffusion limit $n \rightarrow \infty$ with the scaling of the transition probabilities given below. Fig. 1c shows the relationship between the random walk sites and the state diagram of the interval model. Subintervals are demarcated by vertical lines. A diffuser in subinterval i is represented by a walker occupying site i at the midpoint of the subinterval.

Site s represents the single-occupancy binding site and site d represents the “dead” state. Entrance into d models conversion of the diffusing substrate into a product and immediate product release from the binding site. These products are assumed not to reoccupy the binding site s and not to interfere with other substrate molecules binding the site s .

2.1. Transition probabilities

To construct the interval model, first define notation for random variables and expectations associated with the random walk. Let $N_i(t) \in \{0, 1, 2, \dots\}$ for $1 \leq i \leq n$ denote the number of walkers at site i and time t . $N_s(t) \in \{0, 1\}$ denotes the number of walkers at the single-occupancy binding site. Let $M_i(t) = E[N_i(t)]$ and $M_s(t) = E[N_s(t)]$, where the expectations are taken with respect to an ensemble of identically prepared systems. Let $x_i = i/n$, for $0 \leq i \leq n$, denote the points that partition the interval in Fig. 1c and let x_i^* , for $1 \leq i \leq n$, denote the midpoint of subinterval i . x_i^* is the coordinate of random walk site i . Approximate the relationship between the random walk occupation probabilities, $M_i(t)$, and the concentration of the limiting diffusion process, $c(x, t)$, by

$$M_i(t) = c(x_i^*, t) \Delta x, \tag{4}$$

where $\Delta x = x_i - x_{i-1} = 1/n$.

Consider a discrete-time random walk with transitions at $t = t_0, t_0 + \Delta t, t_0 + 2\Delta t, \dots$. Transition probabilities between neighboring sites i and j in the interval are given by

$$k_{i \rightarrow j} = \Delta t n^2, \tag{5}$$

where $1 \leq i, j \leq n$. This scaling with n yields the diffusion equation. Transition probabilities from the single-occupancy site s to the neighboring sites d and 1 are given by

$$k_{s \rightarrow d} = \Delta t \kappa_{s \rightarrow d}, \tag{6}$$

$$k_{s \rightarrow 1} = \Delta t \kappa_{s \rightarrow 1}, \tag{7}$$

where the transition rates $\kappa_{s \rightarrow d}$ and $\kappa_{s \rightarrow 1}$ are independent of n and Δt . The time step scales with n according to $\Delta t = \Delta \tau / n^2$, with $\Delta \tau$ independent of n . Note that Δt scales with n like Δx^2 and that $\Delta \tau$ can be chosen so that each $|k_{i \rightarrow j}| \leq 1$. The transition probabilities and rates are assumed to be independent of the initial time step t_0 .

The probability that a walker initially at site s at time t_0 will remain at site s through the next m time steps is $[1 - (\kappa_{s \rightarrow 1} + \kappa_{s \rightarrow d})]^m$. In the diffusion limit $n \rightarrow \infty$, the probability that the walker will remain on the site s for at least a fixed time t is

$$\lim_{n \rightarrow \infty} \left[1 - (\kappa_{s \rightarrow d} + \kappa_{s \rightarrow 1}) \frac{t}{m} \right]^m = \exp[-(\kappa_{s \rightarrow 1} + \kappa_{s \rightarrow d})t], \tag{8}$$

where $t = m\Delta t$ and $m \propto n^2$. In the diffusion limit, transitions out of the binding site s are exponentially distributed in time. Physically, one expects that a diffuser entering a binding site often will have to surmount a Gibbs free energy barrier. This could be due to the requirement that the diffuser have a particular orientation on entrance, which would involve a decrease of entropy. Exponentially distributed transition densities are found in the high friction limit of Kramers' theory of diffusive escape over a potential energy barrier (Kramers, 1940; Risken, 1989). This theory requires that the binding site s correspond to a well-defined energy minimum and that the barrier is several $k_B T$ in height.

Next investigate how $k_{1 \rightarrow s}$ scales with n . In order for the interval model to be physically consistent, it must satisfy detailed balance at thermodynamic equilibrium (Elston and Doering, 1996). The detailed balance condition between random walk sites s and 1 is:

$$M_s k_{s \rightarrow 1} = M_1 k_{1 \rightarrow s}. \tag{9}$$

The transition probability $k_{s \rightarrow 1}$ depends on n only through Δt . M_s remains finite and positive in the limit $n \rightarrow \infty$. But $M_1 \propto n^{-1}$, since it represents the probability that a diffuser will be in a subinterval of width Δx . Therefore

$$k_{1 \rightarrow s} = \Delta t n \kappa_{1 \rightarrow s} \tag{10}$$

with the rate $\kappa_{1 \rightarrow s}$ independent of n and Δt .

2.2. *Boundary conditions of the interval model*

Assume that the values of N_s , N_1 and N_2 are known at an initial time t . The average change in N_1 over the next time step is given by

$$\begin{aligned} E[N_1(t + \Delta t) - N_1(t)|N_s(t), N_1(t), N_2(t)] \\ = N_2k_{2 \rightarrow 1} - N_1k_{1 \rightarrow 2} + N_s k_{s \rightarrow 1} - N_1(1 - N_s)k_{1 \rightarrow s}, \end{aligned} \tag{11}$$

where the last term models entrance into the binding site from the interval. If $N_s = 0$, an entrance can take place with probability $N_1k_{1 \rightarrow s}$. However, if $N_s = 1$ then no entrance takes place. Average over the ensemble to get

$$M_1(t + \Delta t) - M_1(t) = M_2k_{2 \rightarrow 1} - M_1k_{1 \rightarrow 2} + M_s k_{s \rightarrow 1} - M_1k_{1 \rightarrow s} + M_{1s}k_{1 \rightarrow s}, \tag{12}$$

where $M_{1s} = E[N_1N_s]$. Substitute the scaling between M_i and $c(x_i^*, t)$, (4), and the expressions for the transition probabilities, (5), (7) and (10), divide by Δt and let $n \rightarrow \infty$ to obtain

$$-\frac{\partial c}{\partial x}(0, t) = M_s \kappa_{s \rightarrow 1} - c(0, t)\kappa_{1 \rightarrow s} + \left(\lim_{n \rightarrow \infty} n M_{1s} \right) \kappa_{1 \rightarrow s}. \tag{13}$$

Note that the left-hand side of (12) is proportional to Δx through (4). After dividing by Δt , the limit $n \rightarrow \infty$ gives 0. Comparing the expression on the left of (13) with (3), we see that this is an expression for the net flux out of the binding site into the interval. The first term on the right gives the unidirectional flux out of the binding site and the next two terms give the counter-flux. The term proportional to M_{1s} models entrances that are frustrated by the single-occupancy constraint, decreasing the counter-flux.

The average change in N_s over the time step following the initial time t is given by

$$E[N_s(t + \Delta t) - N_s(t)|N_s(t), N_1(t)] = N_1(1 - N_s)k_{1 \rightarrow s} - N_s(k_{s \rightarrow 1} + k_{s \rightarrow d}). \tag{14}$$

Average over the ensemble to obtain

$$M_s(t + \Delta t) - M_s(t) = M_1k_{1 \rightarrow s} - M_{1s}k_{1 \rightarrow s} - M_s(k_{s \rightarrow 1} + k_{s \rightarrow d}). \tag{15}$$

Substitute the scaling between M_1 and $c(x_1^*, t)$ and the expressions for transition probabilities, divide by Δt and let $n \rightarrow \infty$ to obtain

$$M'_s(t) = c(0, t)\kappa_{1 \rightarrow s} - \lim_{n \rightarrow \infty} (n M_{1s})\kappa_{1 \rightarrow s} - M_s(\kappa_{s \rightarrow 1} + \kappa_{s \rightarrow d}). \tag{16}$$

The right-hand side of this equation includes all of the terms on the right-hand side of (13), prefixed by a minus sign. The additional term, $-M_s \kappa_{s \rightarrow d}$, is due to transitions into the dead state.

A boundary condition for the diffusion equation at $x = 1$ can be obtained by a similar argument. Refer to Fig. 1b. The average change in N_n over the time step from t to $t + \Delta t$ is given by

$$E[N_n(t + \Delta t) - N_n(t)|N_{n-1}(t), N_n(t)] = N_{n-1}(t)k_{n-1 \rightarrow n} - N_n(t)k_{n \rightarrow n-1}. \tag{17}$$

Average over the ensemble, substitute the midpoint rule scaling and the expressions for transition probabilities, divide by Δt and let $n \rightarrow \infty$ to obtain

$$0 = -\frac{\partial c}{\partial x}(1, t) = j(1, t), \quad (18)$$

using (3). This boundary condition, which corresponds to reflection of trajectories at $x = 1$, is easily constructed from the diffusion limit of a random walk.

The interval model consists of the diffusion equation, (2), coupled with the equation for the time evolution of M_s , (16), through the single-occupancy boundary condition, (13). It also includes the reflecting boundary condition, (18). As it stands, this system of equations is not closed because of its dependence on the joint expectation M_{1s} .

2.3. The high D limit

The interval model simplifies in the limit of large diffusion coefficient. In particular, one obtains an expression for M_{1s} in terms of M_1 and M_s that closes the interval model.

First consider three useful expressions that are valid for all values of D . Since N_s has only two possible states

$$M_s = E[N_s] = \Pr\{N_s = 1\}. \quad (19)$$

Using the properties of conditional expectation

$$M_{1s} = E[N_1 N_s] = E[N_1 | N_s = 1] E[N_s]. \quad (20)$$

Using the law of total probability for expectations

$$\begin{aligned} M_1 &= E[N_1 | N_s = 0] \Pr\{N_s = 0\} + E[N_1 | N_s = 1] \Pr\{N_s = 1\} \\ &= E[N_1 | N_s = 0](1 - M_s) + E[N_1 | N_s = 1] M_s. \end{aligned} \quad (21)$$

What does the limit $D \rightarrow \infty$ correspond to in the interval model, using dimensionless variables? Assume that the dimensional rates of entrance and escape from the site s , with physical units of inverse time, are independent of the diffusion coefficient D in the interval. Denote these rates $K_{s \rightarrow 1}$ etc. The dimensionless rates are defined by

$$\kappa_{s \rightarrow 1} = t'_D K_{s \rightarrow 1}, \quad (22)$$

etc. As $D \rightarrow \infty$, $t'_D \rightarrow 0$; the limit thus corresponds to infinitesimal values for $\kappa_{s \rightarrow 1}$, etc. That is, the mean time required for the diffuser to enter or leave the binding site becomes much longer than the mean time required for it to diffuse across the interval. Then make an approximation which is reminiscent of adiabatic elimination (for example, Gardiner, 1983). Assume that the fast process (time evolution of particle concentration in the interval) relaxes to a value given by taking the state of the slow process (time evolution of binding site occupation) as constant. Without a change in the occupation of the binding site, the concentration of diffusers in the interval would relax to a constant. Therefore,

assume that the concentration of diffusers in the interval is constant. Let M_I be the mean number of diffusers in the interval:

$$M_I(t) = \int_0^1 c(x, t) dx. \quad (23)$$

In the high D limit, $M_I = M_I/n$.

2.3.1. Subcase $k_{s \rightarrow d} = 0$

Assume that entrance into the dead state is not possible. Let n_W be the total number of walkers in the random walk of Fig. 1b. Then

$$N_I + N_s = n_W, \quad (24)$$

where N_I is the number of diffusers in the interval. We then have

$$E[N_I | N_s = 0] = n_W/n, \quad (25)$$

$$E[N_I | N_s = 1] = (n_W - 1)/n. \quad (26)$$

This result reflects the fact that N_I and N_s are anticorrelated. Substitute these expressions into (21) and (20) and eliminate $1/n$ to obtain

$$M_{1s} = \frac{n_W - 1}{n_W - M_s} M_I M_s. \quad (27)$$

This expression for the joint expectation M_{1s} in terms of M_I and M_s closes the interval model. Its form is chosen to make an easy comparison with statistical independence. Since $M_s < 1$, one has $M_{1s} < M_I M_s$. Compared with the result expected if N_s and N_I were independent, their joint expectation is reduced by their anticorrelation. Call this expression for M_{1s} the assumption of *particle number dependence*.

2.3.2. Subcase $k_{s \rightarrow d} > 0$

Now allow the transitions into the dead state. Then

$$N_I + N_s + N_d = n_W. \quad (28)$$

Taking expectations,

$$M_I + M_s + M_d = n_W. \quad (29)$$

Define expected values conditioned on the binding site being occupied

$$\tilde{M}_z = E[N_z | N_s = 1] \quad (30)$$

for $z \in \{I, d, s\}$. Note $\tilde{M}_s = 1$. Then

$$\tilde{M}_I + \tilde{M}_d = n_W - 1. \quad (31)$$

One might expect $\tilde{M}_I < M_I$ and $\tilde{M}_d < M_d$, since the quantities on the left are conditioned on the information that s is occupied, and the total number of particles is fixed.

Approximate $\tilde{M}_I = \alpha_I M_I$, and $\tilde{M}_d = \alpha_d M_d$ with a common $\alpha = \alpha_I = \alpha_d$. Below, this approximation will be studied numerically. From (20) then obtain

$$M_{1s} = \alpha M_1 M_s. \tag{32}$$

From (29) and (31)

$$\alpha(n_W - M_s) = n_W - 1. \tag{33}$$

Solving for α in (33) and substituting the result into (32) brings us back to particle number dependence, (27). For the subcase $\kappa_{s \rightarrow d} = 0$, this holds in the limit $D \rightarrow \infty$. For $\kappa_{s \rightarrow d} > 0$, the approximation made to obtain (27) seems very uncertain. However, numerical evidence will be presented showing that particle number dependence can be accurate in this second subcase.

Lin et al. (1990) have analyzed other moment closure schemes for a system of diffusing and interacting particles on a 1D lattice. These involve the approximate expression of third moments as products of second moments. Particle number dependence is simpler in one sense, the second moment is approximated as a function of first moments, in this way similar to statistical independence. However, the function does not have product form.

Substitute (27) into (13) and use (4) to obtain a boundary condition for the interval model

$$-\frac{\partial c}{\partial x}(0, t) = M_s \kappa_{s \rightarrow 1} - n_W \frac{1 - M_s}{n_W - M_s} c(0, t) \kappa_{1 \rightarrow s}. \tag{34}$$

Similarly, from (16) the time evolution of the binding site occupation probability becomes

$$M'_s(t) = n_W \frac{1 - M_s}{n_W - M_s} c(0, t) \kappa_{1 \rightarrow s} - M_s (\kappa_{s \rightarrow 1} + \kappa_{s \rightarrow d}). \tag{35}$$

2.3.3. *The two variable approximation*

The interval model can be simplified further by making the following replacements which approximate the concentration of diffusers in the interval as a constant

$$\hat{c}(t) = c(x, t), \quad \text{for } 0 \leq x \leq 1, \tag{36}$$

$$\frac{d\hat{c}}{dt} = -\frac{\partial c}{\partial x}(0, t). \tag{37}$$

In the second of these equations, the expressions on the left and right-hand sides both give the rate at which the number of diffusers in the interval is increasing. The form on the right is the probability flux into the interval due to Fick's law. Making these substitutions into (34) and (35) simplifies the interval model to

$$\hat{c}'(t) = M_s(t) \kappa_{s \rightarrow 1} - n_W \frac{1 - M_s(t)}{n_W - M_s(t)} \hat{c}(t) \kappa_{1 \rightarrow s}, \tag{38}$$

$$M'_s(t) = n_W \frac{1 - M_s(t)}{n_W - M_s(t)} \hat{c}(t) \kappa_{1 \rightarrow s} - M_s(t) (\kappa_{s \rightarrow 1} + \kappa_{s \rightarrow d}). \tag{39}$$

This *two variable approximation* is a pair of coupled first order, nonlinear, ordinary differential equations. The physical domain is the semiinfinite strip $\{0 \leq M_s \leq 1, \hat{c} \geq 0\}$. The origin of the (M_s, \hat{c}) plane is a fixed point. On the half-open interval $\{0 < M_s \leq 1, \hat{c} = 0\}$, (38) gives $\hat{c}' > 0$. On the half-line $\{M_s = 0, \hat{c} > 0\}$, (39) gives $M'_s > 0$. On the half-line $\{M_s = 1, \hat{c} > 0\}$, (39) gives $M'_s < 0$. Therefore the physical domain is invariant under the flow. The qualitative character of the flow depends on whether $k_{s \rightarrow d} = 0$ or $k_{s \rightarrow d} > 0$.

For the subcase $k_{s \rightarrow d} = 0$, fixed points satisfy the equation obtained by setting the right-hand side of (38) or (39) equal to zero. In addition, the total number of particles is conserved, giving

$$\hat{c}(t) + M_s(t) = n_w \tag{40}$$

where n_w is determined by the initial condition. These two equations determine the fixed point that the system approaches as $t \rightarrow \infty$. We obtain

$$M_s(\infty) = n_w \kappa_{1 \rightarrow s} / (\kappa_{s \rightarrow 1} + n_w \kappa_{1 \rightarrow s}), \tag{41}$$

and $\hat{c}(\infty) = n_w - M_s(\infty)$. When $n_w = 1$, this result is the same as for a two state Markov process with transition rates $\kappa_{s \rightarrow 1}$ and $\kappa_{1 \rightarrow s}$. In general, flow is from the initial condition in the physical domain, along the line given by (40), and toward the fixed point, which represents a physical steady state. This flow is sketched in Fig. 2a.

For the subcase $k_{s \rightarrow d} > 0$, add (38) to (39) to obtain

$$\hat{c}'(t) + M'_s(t) = -M_s(t) \kappa_{s \rightarrow d} < 0. \tag{42}$$

From this result, we obtain that the only steady state is $(M_s, \hat{c}) = (0, 0)$. Furthermore, the closed domain bounded by the interval $\{0 \leq M_s \leq 1, \hat{c} = 0\}$ and the lines $M_s = 0$, $M_s = 1$ and $\hat{c} + M_s = n_w$ (where $n_w = \hat{c}(0) + M_s(0)$) is invariant under the flow. In view of (42), there can be no closed orbits in this region. From the generalized Poincaré–Bendixson theorem (Perko, 2001), it follows that all trajectories much approach the origin as $t \rightarrow \infty$. This flow is sketched in Fig. 2b.

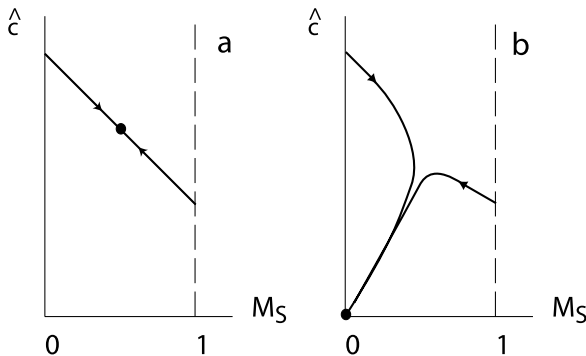


Fig. 2 (a) Flow of interval model for $k_{s \rightarrow d} = 0$. (b) Flow of interval model for $k_{s \rightarrow d} > 0$.

2.4. Simulation results

The interval model is simulated using an implementation of the discrete time random walk described above, with walkers making transitions between sites which represent the subinterval midpoints. At each fractional time step, $\Delta t_f = \Delta t/n_w$, a random number is generated to choose a walker and then a second random number is generated to choose its transition, using the transition probabilities obtained above. This algorithm is not as efficient as the continuous time random walk algorithm described by Gillespie (1977), particularly when transition rates involve a wide range of time scales. However, discrete time random walks provide a simple setting for deriving the interval model and use of a discrete time simulation algorithm is consistent.

For each case, the initial condition corresponds to $n_w = 2$ walkers placed randomly on a 1D lattice of $n = 8$ sites; see Fig. 1c. In the analysis above, the $D \rightarrow \infty$ limit corresponds to infinitesimal values of $\kappa_{1 \rightarrow s}$, $\kappa_{s \rightarrow 1}$ and $\kappa_{s \rightarrow d}$. Random walk simulations (Runs) 1 and 2 are made with $\kappa_{s \rightarrow d} = 0$, simulating a diffuser entering and leaving a binding site, but without conversion into product. In the $D \rightarrow \infty$ limit the analysis of the interval model shows that the joint probability M_{1s} will be given by the particle number dependence expression, (27). Runs 3 and 4 are made with $\kappa_{s \rightarrow d} > 0$. In the $D \rightarrow \infty$ limit, the particle number dependence expression for M_{1s} is only obtained as an uncontrolled approximation. When this expression for M_{1s} does hold the two variable approximation, (38) and (39), is obtained.

In Fig. 3, the first 2 panels of each row show M_I and M_s as a function of time. Dots show $\langle N_I \rangle$ and $\langle N_s \rangle$ where $\langle \dots \rangle$ denotes the average over simulations. Solid curves show results of numerically integrating the two variable approximation. In the last panel of each row, dots show $\langle N_I N_s \rangle \approx M_{1s}$. The lower curve shows the particle number dependence approximation, (27), and the upper curve shows the assumption of independence, $M_{1s} = M_I M_s$. To construct both of these approximate curves, values of M_I and M_s used are averages over simulations as described above.

Run 1 uses $\kappa_{1 \rightarrow s} = 1$, $\kappa_{s \rightarrow 1} = 1$ and $\kappa_{s \rightarrow d} = 0$ with 4×10^4 simulations made over a model time of $4t_D^*$. Results are presented in the first row of Fig. 3. The first two panels show M_I decreasing from an initial value of 2 and M_s increasing from 0 with their sum fixed at $n_w = 2$. There is a significant discrepancy with the behavior of the two variable model. Panel (c) shows a small discrepancy between the simulated values of M_{1s} and particle number dependence for $t < 1$. However, particle number dependence gives a much better approximation to the simulated results than independence.

Although the analysis of the limit $D \rightarrow \infty$ corresponds to infinitesimal values for $\kappa_{1 \rightarrow s}$, $\kappa_{s \rightarrow 1}$ and $\kappa_{s \rightarrow d}$, the numerical simulations suggest that particle number dependence and the two variable approximation are in close agreement with the interval model if only $\kappa_{1 \rightarrow s} \ll 1$; $\kappa_{s \rightarrow 1}$ and $\kappa_{s \rightarrow d}$ may be $\mathcal{O}(1)$. Run 2 uses $\kappa_{1 \rightarrow s} = 1/16$, $\kappa_{s \rightarrow 1} = 1$ and $\kappa_{s \rightarrow d} = 0$. Results shown in the second row of Fig. 3 are averages of 1.6×10^5 simulations. Large numbers of simulations were required in runs 2 and 4 in order to obtain accurate estimates of M_{1s} , since simultaneous occupation of sites 1 and s was rare. For run 2, simulated averages of M_I and M_s are in excellent agreement with the two variable approximation and simulated averages of M_{1s} are in excellent agreement with particle number dependence.

Run 3 uses $\kappa_{1 \rightarrow s} = 1$, $\kappa_{s \rightarrow 1} = 1$ and $\kappa_{s \rightarrow d} = 1$. With $\kappa_{s \rightarrow d} > 0$, all of the walkers eventually enter the state d of Fig. 1. Results shown in the third row of Fig. 3 are averages of 4×10^4 simulations. M_I decreases from its initial value of 2 to 0 as $t \rightarrow \infty$. M_s and M_{1s}

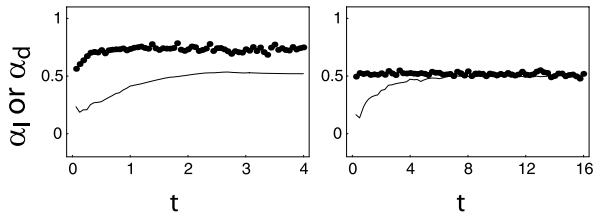


Fig. 4 α_I and α_d as a function of time calculated from simulations of the interval model. Dots show values of α_I and the solid curves show values of α_d . (a) Results from Run 3. (b) Results from Run 4.

Corresponding to runs 1 through 4, which use $n_w = 2$, a set of runs have been made with the same values for the transition rates but with $n_w = 5$ (not shown). The differences between the results of these runs and those in Fig. 3 can also be understood, in part, in terms of the prefactor of $M_1 M_s$. The $n_w = 5$ runs made with the smaller value of $\kappa_{1 \rightarrow s}$ again follow the particle number dependence curves closely. However, the relative differences of values between the particle number dependence and statistical independence curves are smaller for $n_w = 5$ compared with $n_w = 2$. For the $n_w = 5$ run corresponding to run 1, M_s increases to values above 0.8. The relative difference ((larger-smaller)/smaller) between particle number dependence and statistical independence is less than 5%. For the $n_w = 5$ run corresponding to run 2, values of M_s remain smaller and the relative difference between particle number dependence and statistical independence is approximately 20%.

For a physical perspective, consider the cartoon of a thylakoid membrane microdomain mentioned in the introduction (Kirchhoff et al., 2000). The domain includes 5 to 10 plastoquinone molecules and 6 plastoquinone binding sites. At any one time, some of the plastoquinone may be bound, reducing the concentration of free plastoquinone available to an open binding site. The binding and unbinding transition rates are not known. If binding to all of these sites is tight, the effective value of n_w would be relatively small, but the value of M_s for each site would be relatively large, and conversely if binding is loose. In this way, effects of n_w and M_s on the particle number dependence prefactor may partially cancel.

3. The spherical model

This section considers diffusion in a simple unbounded domain. Begin by considering the problem with physical dimensions. Let R be the radial coordinate in a spherical coordinate system and consider diffusion in the domain $R > A$, with spherical symmetry and a single-occupancy binding site at $R = A$. The diffusion equation with spherical symmetry is

$$\frac{\partial C}{\partial t'} = D \frac{1}{R^2} \frac{\partial}{\partial R} \left(R^2 \frac{\partial C}{\partial R} \right), \quad (43)$$

where $[R] = \text{length}$, $[t'] = \text{time}$, $[C] = \text{length}^{-3}$ and $[D] = \text{length}^2/\text{time}$. Introduce a dimensionless spatial coordinate $r = R/A$ and time $t = t'/t'_D$, where $t'_D = A^2/D$ is the

diffusive time scale. Let the dimensionless concentration be $c(r, t) = A^3 C(R, t')$. Obtain the diffusion equation in dimensionless variables

$$\frac{\partial c}{\partial t} = \frac{1}{r^2} \frac{\partial}{\partial r} \left(r^2 \frac{\partial c}{\partial r} \right). \tag{44}$$

Replace concentration by the probability density $p(r, t) = 4\pi r^2 c(r, t)$ to obtain the Smoluchowski equation

$$\frac{\partial p}{\partial t} = \frac{\partial}{\partial r} \left(\frac{-2}{r} p + \frac{\partial p}{\partial r} \right). \tag{45}$$

The first term on the right-hand side is a drift associated with the potential

$$w(r) = -2 \ln(r). \tag{46}$$

The fictitious force $-w'(r)$ models the systematic tendency of a diffuser to drift away from the origin of spherical coordinates. The Smoluchowski equation also has the form of an equation of continuity $\partial p / \partial t = -\partial j / \partial r$, where the dimensionless probability current j has the form

$$j = \frac{2}{r} p - \frac{\partial p}{\partial r}. \tag{47}$$

This includes a component proportional to the fictitious force and a Fick's law contribution.

The spherical model includes the Smoluchowski equation in the spherical shell $a = 1 < r < b$ with a single-occupancy boundary condition at $r = 1$. The endpoint $r = b$ corresponds to $R = Ab$. Fig. 5a shows the state diagram. Diffusers can enter the binding site s from the shell at $r = 1$ and then escape from s back into the shell, or be converted

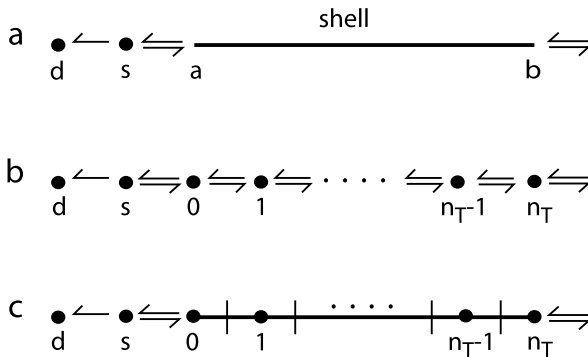


Fig. 5 (a) State diagram of the spherical model. Diffusion takes place on the shell $a = 1 < r < b$. s is the single-occupancy binding site. The transition $s \rightarrow d$ signifies conversion of substrate to product, immediately followed by release of product. (b) Random walk n of the sequence whose limit is the spherical model. (c) Random walk sites are related to subintervals of the shell in a manner similar to the trapezoid rule of numerical integration.

into product and then immediately released. This latter step is modeled by a transition to the state d . Assume that product molecules do not reenter the binding site and do not interfere with other substrate molecules entering the binding site. Diffusers can also enter or leave the shell at $r = b$, corresponding to the interface between the shell and an infinite bulk in the region $\{r > b\}$. The spherical model is constructed as the limit of a sequence of random walks. Fig. 5b shows the n th random walk in this sequence. There are n random walk sites per unit length in the shell, for a total of $n_T + 1$ sites in the shell, with $n_T = n(b - 1)$.

Fig. 5c shows the correspondence between the random walk sites and the spherical shell. Unlike the relationship between the random walks sites and the interval in the interval model, the endmost random walk sites in the shell do not sit at the midpoints of subintervals. Instead, the relationships between the random walk sites and the subintervals is like that of the extended trapezoid rule of numerical integration. One may regard that the sites in the interior of the shell are at the midpoints of their subintervals, but then the endmost sites are at the endpoints of subintervals of half width. Random walk site i is located at $r_i = 1 + i\Delta r$ for $0 \leq i \leq n_T$ and $\Delta r = 1/n$. Midway between these sites are the partition points $r_1^* \cdots r_{n_T}^*$. This "trapezoid rule" is used to obtain numerical results for comparison with the analysis of the spherical model.

Initially, an attempt was made to simulate a spherical model random walk that was constructed using the midpoint rule. In this case the shell, which is delimited by a and b in Fig. 5a, is partitioned like the interval $[0, 1]$ of Fig. 1a, as shown by Fig. 1c. Convergence to the $n \rightarrow \infty$ limit was found to be very slow. The random walk based on the midpoint rule models entrances from the shell to the binding site by transitions from $\hat{r}_1 = 1 + 1/(2n)$ to the binding site. But $p(\hat{r}_1, t)$ is significantly different from $p(1, t)$, even in the case of D large, because of the spherical geometry: $p(r, t) = 4\pi r^2 c(r, t)$. The geometric factor introduces an $\mathcal{O}(1/n)$ error into the entrance rate. The trapezoid rule places random walk sites at the endpoints $r = a$ and $r = b$, avoiding this error.

3.1. Transition probabilities in the shell and at the binding site

Let $N_i(t) \in \{0, 1, 2, \dots\}$ for $0 \leq i \leq n_T$ denote the number of walkers at site i and time t . $N_s(t) \in \{0, 1\}$ denotes the number of walkers at the single-occupancy binding site. Let $M_i(t) = E[N_i(t)]$ and $M_s(t) = E[N_s(t)]$. Assume the relationship between the random walk occupation probabilities, $M_i(t)$, and the probability density of the limiting diffusion process, $p(r, t)$, is given by

$$M_i(t) = \begin{cases} p(r_i, t)\Delta r/2, & \text{for } i = 0, n_T, \\ p(r_i, t)\Delta r, & \text{for } 1 \leq i \leq n_T - 1. \end{cases} \quad (48)$$

This approximation is somewhat delicate at the endmost sites, representing intervals of half width, and is discussed in the summary and discussion.

To obtain transition probabilities for the random walk on the shell, use the Agmon–Hopfield formula for neighboring sites i and j in the shell (Agmon and Hopfield, 1983). The general form is

$$k_{i \rightarrow j} = \Delta t n^2 e^{(w_i - w_j)/2}, \quad (49)$$

where $w_i = w(r_i)$ is a potential associated with a Smoluchowski equation. As with the interval model, $\Delta t = \Delta\tau/n^2$ with $\Delta\tau$ independent of n . Then $\Delta\tau$ may be chosen so that $\max(k_{i \rightarrow j}) \leq 1$. The Agmon–Hopfield formula may be obtained by requiring that the transition probabilities satisfy detailed balance and are consistent with the Boltzmann distribution at thermodynamic equilibrium, and that the corresponding master equation gives a finite difference approximation to the Smoluchowski equation (Elston and Doering, 1996). It can be generalized to state-dependent diffusion coefficients (Bernèche and Roux, 2003) and to two spatial variables (Schumaker and Watkins, 2004). Recently, other expressions for transition rates which satisfy detailed balance and lead to the Smoluchowski equation have been proposed (Wang and Peskin, 2003; Xing et al., 2005). When the effective potential for radial diffusion, (46), is substituted into (49), one obtains

$$k_{i \rightarrow j} = \begin{cases} 2\Delta tn^2(r_j/r_i), & \text{for } i = 0, n_T, \\ \Delta tn^2(r_j/r_i), & \text{for } 1 \leq i \leq n_T - 1, \end{cases} \tag{50}$$

where the factor of two is introduced because sites 0 and n_T represent shell subintervals of half width. The rates for leaving the endmost sites are doubled with the result that the expected number of walkers on those sites is halved.

Transition probabilities from the single-occupancy site s to the neighboring sites 0 and d scale with n and Δt in the same way as those for the interval model; see (6) and (7) with interval model site 1 replaced by spherical model site 0. In the limit $n \rightarrow \infty$, these expressions lead to transition densities which are exponentially distributed in time. Similar to the derivation of (10), detailed balance leads to

$$k_{0 \rightarrow s} = 2\Delta tn\kappa_{0 \rightarrow s}, \tag{51}$$

where the factor of two appears because site 0 represents a subinterval of half width. The binding site s can be occupied by at most one diffuser. Entrance into s at time $t_0 + \Delta t$ can only occur if it is empty at time t_0 .

3.2. Boundary condition at the binding site

Assume that the values of N_s , N_0 and N_1 are known at an initial time t . The average change in N_0 over the next time step is given by

$$\begin{aligned} & E[N_0(t + \Delta t) - N_0(t) | N_s(t), N_0(t), N_1(t)] \\ &= N_1 k_{1 \rightarrow 0} - N_0 k_{0 \rightarrow 1} + N_s k_{s \rightarrow 0} - N_0(1 - N_s) k_{0 \rightarrow s}. \end{aligned} \tag{52}$$

Average over the ensemble to get

$$M_0(t + \Delta t) - M_0(t) = M_1 k_{1 \rightarrow 0} - M_0 k_{0 \rightarrow 1} + M_s k_{s \rightarrow 0} - M_0 k_{0 \rightarrow s} + M_{0s} k_{0 \rightarrow s}, \tag{53}$$

where $M_{0s} = E[N_0 N_s]$. Substitute the scaling between M_i and $p(r_i, t)$, (48), and the expressions for the transition probabilities, divide by Δt and let $n \rightarrow \infty$ to obtain

$$2p(1, t) - \frac{\partial p}{\partial r}(1, t) = M_s(t)\kappa_{s \rightarrow 0} - p(1, t)\kappa_{0 \rightarrow s} + \left(\lim_{n \rightarrow \infty} 2nM_{0s} \right) \kappa_{0 \rightarrow s}. \tag{54}$$

Comparing the expression on the left with (47), we see that this is an expression for the net flux out of the binding site and into the shell at $r = 1$. This boundary condition is analogous to (13).

The average change in N_s over the time step following the initial time t is given by

$$E[N_s(t + \Delta t) - N_s(t) | N_s(t), N_0(t)] = N_0(1 - N_s)k_{0 \rightarrow s} - N_s(k_{s \rightarrow 0} + k_{s \rightarrow d}). \quad (55)$$

Average over the ensemble to obtain

$$M_s(t + \Delta t) - M_s(t) = M_0 k_{0 \rightarrow s} - M_{0s} k_{0 \rightarrow s} - M_s(k_{s \rightarrow 0} + k_{s \rightarrow d}). \quad (56)$$

Substitute the scaling between M_i and $p(r_i, t)$ and the expressions for transition probabilities, divide by Δt and let $n \rightarrow \infty$ to obtain

$$M'_s(t) = p(1, t)\kappa_{0 \rightarrow s} - \lim_{n \rightarrow \infty} (2nM_{0s})\kappa_{0 \rightarrow s} - M_s(t)(\kappa_{s \rightarrow 0} + \kappa_{s \rightarrow d}). \quad (57)$$

The right-hand side of this equation contains all of the terms on the right-hand side of (54), prefixed by a minus sign. The additional term, $-M_s\kappa_{s \rightarrow d}$, is due to the transition into the dead state.

3.3. Transition probabilities between the shell and the bulk

Nadler et al. (2001) studied the stationary arrival process of infinitely many new, identical, independent diffusers from an infinite bath to a smooth absorbing boundary. The diffusers are new in the sense that they have not visited the absorbing boundary previously. Those authors obtained the very simple and general result that arrival times are exponentially distributed. Our boundary condition models this result in the special case of absorption to a sphere of radius b .

Consider spherically symmetric diffusion outside a sphere of radius b . Let $c_{SS}(r)$ be the steady-state concentration of diffusing particles in this region—the solution of (44) with zero time derivative. The steady state solution satisfying $c_{SS}(b) = 0$ and with $c_{SS}(r) \rightarrow c_0$ as $r \rightarrow \infty$ is given by $c_{SS}(r) = c_0(1 - b/r)$. The total flux into the sphere is then $4\pi b^2 c'_{SS}(b) = 4\pi b c_0$. Model this flux in the random walk of Fig. 5b by defining the probability of arrival of new particles from the bulk into the shell, per time step

$$k_{B \rightarrow n_T} = \Delta t \kappa_{B \rightarrow n_T}, \quad \text{where } \kappa_{B \rightarrow n_T} = 4\pi b c_0. \quad (58)$$

In the limit $n \rightarrow \infty$ we obtain a Poisson process of new arrivals. $k_{B \rightarrow n_T}$ is not a transition probability from a random walk site representing the bulk; no sites model the bulk in the Spherical Model. Instead, $k_{B \rightarrow n_T}$ models a constant probability of arrival per time step.

In order for the spherical model to be physically consistent, it must satisfy detailed balance at thermodynamic equilibrium (Elston and Doering, 1996). Detailed balance requires that the rate at which particles leave the shell from site n_T must be equal to the rate of arrivals:

$$M_{n_T} k_{n_T \rightarrow B} = 4\pi b c_0 \Delta t, \quad (59)$$

where $M_{n_T} = V_{n_T} c_0$ and V_{n_T} is the volume of the subshell associated with the site n_T . Note that, at equilibrium, the concentration of diffusers is c_0 everywhere. Then obtain

$$k_{n_T \rightarrow B} = \frac{4\pi b \Delta t}{V_{n_T}} = \frac{2n}{b} \Delta t (1 + \mathcal{O}(n^{-1})). \quad (60)$$

This transition step corresponds to particles disappearing from the random walk at site n_T . Under steady-state conditions, and in the limit $n \rightarrow \infty$, these escapes are exponentially distributed in time. They correspond to diffusers which are lost from the shell forever and must balance the rates at which diffusers newly arrive to the shell from the bulk.

The transition probabilities given by (58) and (60) take into account particles that have newly arrived from the bulk to the shell and particles that are lost from the shell forever. However, they ignore particles that escape from the shell to the bulk and then return. In a second paper, Nadler et al. (2003) present an analysis of these reentering particles and describe an infinite sum of renewal processes that models their behavior in the general time-dependent case. The following section shows that our approach, which ignores reentrances, leads to a simple boundary condition which is satisfied by the time-independent steady states of the spherical model. The last paragraph of the summary and discussion explains why reentering particles do not contribute to the steady state concentration.

3.4. Boundary condition between the shell and the bulk

The change in M_{n_T} over the time step from t to $t + \Delta t$ is given by

$$\begin{aligned} M_{n_T}(t + \Delta t) - M_{n_T}(t) \\ = M_{n_T-1}(t)k_{n_T-1 \rightarrow n_T} + k_{B \rightarrow n_T} - M_{n_T}(t)(k_{n_T \rightarrow n_T-1} + k_{n_T \rightarrow B}). \end{aligned} \quad (61)$$

A boundary condition will be obtained in the limit $n \rightarrow \infty$. First consider one component of this limit

$$L = \lim_{n \rightarrow \infty} \frac{M_{n_T-1}k_{n_T-1 \rightarrow n_T} - M_{n_T}k_{n_T \rightarrow n_T-1}}{\Delta t}. \quad (62)$$

Substitute the scaling between M_i and $p(r_i, t)$, (48), and the expressions for the transition probabilities, (50), and take the limit to obtain

$$L = -\frac{\partial p}{\partial r}(b, t) + \frac{2}{b}p(b, t). \quad (63)$$

Comparing the right-hand side this equation with (47), one sees $L = j(b, t)$. This result is not surprising in view of the form of the difference quotient on the right-hand side of (62). Now divide (61) by Δt , substitute from (48), (58) and (60), and let $n \rightarrow \infty$ to obtain the boundary condition at $r = b$

$$p(b, t) - b \frac{\partial p}{\partial r}(b, t) = -4\pi b^2 c_0. \quad (64)$$

Consider a steady-state solution, $c_{SS}(r)$, of the spherically symmetric diffusion equation, (44), satisfying $c_{SS}(f) = 0$ for some fixed $0 \leq f < b$, and $c_{SS}(r) \rightarrow c_0$ as $r \rightarrow \infty$.

The solution is $c_{SS}(r) = c_0(1 - f/r)$. Substitution shows that (64) is satisfied by the corresponding probability density $p_{SS}(r) = 4\pi r^2 c_{SS}(r)$ for an arbitrary f . This result shows that the boundary condition, (64), corresponds to the approximation that the system is at steady-state at the interface between the shell and the bulk. The boundary condition allows that the system may be pulled away from thermodynamic equilibrium at the outer boundary of the simulated domain. Equation (64) may be compared with the Dirichlet boundary condition that concentration at the outer boundary of the simulated domain is equal to the concentration in the bulk (Song et al., 2004). This latter condition assumes the system is not significantly perturbed from thermodynamic equilibrium at the outer boundary. The grand canonical Monte Carlo method of Im et al. (2000) imposes thermodynamic equilibrium at the boundaries of the simulated domain at the level of particle trajectories.

The spherical model consists of the diffusion equation, (45), coupled with the equation for the time evolution of M_s , (57), through the single-occupancy boundary condition, (54). It also includes a steady-state boundary condition between the shell and the bulk, (64). This system of equations is not closed because of its dependence on the joint probability M_{0s} .

3.5. The high D limit

Similar to the interval model, the $D \rightarrow \infty$ limit of the spherical model corresponds to infinitesimal values for the transition rates $\kappa_{0 \rightarrow s}$, $\kappa_{s \rightarrow 0}$ and $\kappa_{s \rightarrow d}$. For very small values of these rates, the time between particle entrances into the binding site is very long. A particle that is in solution close to a binding site after an entrance will thoroughly mix with the bulk and correlations will decay before the second entrance. The shell approaches equilibrium with the bulk, giving $p(r, t) = 4\pi r^2 c_0$, and N_0 and N_s become statistically independent. This gives $M_{0s} = E[N_0 N_s] = M_0 M_s$ and, using (48),

$$\lim_{n \rightarrow \infty} 2n M_{0s} = 4\pi c_0 M_s. \quad (65)$$

Substitution into (57) yields

$$M'_s(t) + (4\pi c_0 \kappa_{0 \rightarrow s} + \kappa_{s \rightarrow 0} + \kappa_{s \rightarrow d}) M_s(t) = 4\pi c_0 \kappa_{0 \rightarrow s}, \quad (66)$$

which has a simple exact solution. Refer to this as the $D \rightarrow \infty$ solution. Although we have obtained this result only for infinitesimal values of the transition rates, the numerical results below show that this approximation remains accurate when only $\kappa_{0 \rightarrow s}$ is small.

When, in addition, $\kappa_{s \rightarrow d} = 0$, M_s converges to the prediction of the Langmuir absorption isotherm as $t \rightarrow \infty$:

$$M_s(\infty) = \frac{c_0}{c_0 + K_d}, \quad \text{where } K_d = \frac{\kappa_{s \rightarrow 0}}{4\pi \kappa_{0 \rightarrow s}} \quad (67)$$

is the dissociation constant. The geometrical factor of 4π is due to the definition of the on rate in terms of probability density: $p(1, \infty) \kappa_{0 \rightarrow s} = 4\pi c_0 \kappa_{0 \rightarrow s}$.

3.6. Simulation results

The computer code is an implementation of the discrete time random walk described above, with walkers making transitions between the ‘‘trapezoid rule’’ sites of Figs. 5b

and 5c. The discrete time movement algorithm used is the same as that described above for the interval model.

Each run uses $a = 1$, $b = 3$ and $n = 4$, giving $n_T = 8$. The initial condition corresponds to $n_W = 2$ walkers placed randomly in the shell (using the grand canonical ensemble) so that the concentration $c(r, t = 0)$ in the shell is equal to the bulk concentration of $c_0 = 0.01835$. As with the interval model simulations, Runs 1 and 2 are made with $\kappa_{s \rightarrow d} = 0$, simulating a diffuser entering and leaving a binding site, but without conversion into product. Runs 3 and 4 are made with $\kappa_{s \rightarrow d} > 0$. In the $D \rightarrow \infty$ limit, statistical independence of N_s and N_0 gives $M_{0s} = M_0 M_s$, leading to (66) and its solution.

In Fig. 6, the first 2 panels of each row show M_h and M_s as a function of time, where the subscript h refers to the number of walkers in the shell. For this example, $M_h = M_0 + \dots + M_8$. Dots show $\langle N_h \rangle$ and $\langle N_s \rangle$ where $\langle \dots \rangle$ denotes the average over simulations. Solid curves in the middle panels are given by the solution of (66). In the last panel of each row, dots show $\langle N_0 N_s \rangle \approx M_{0s}$. The curve shows the predicted result of statistical

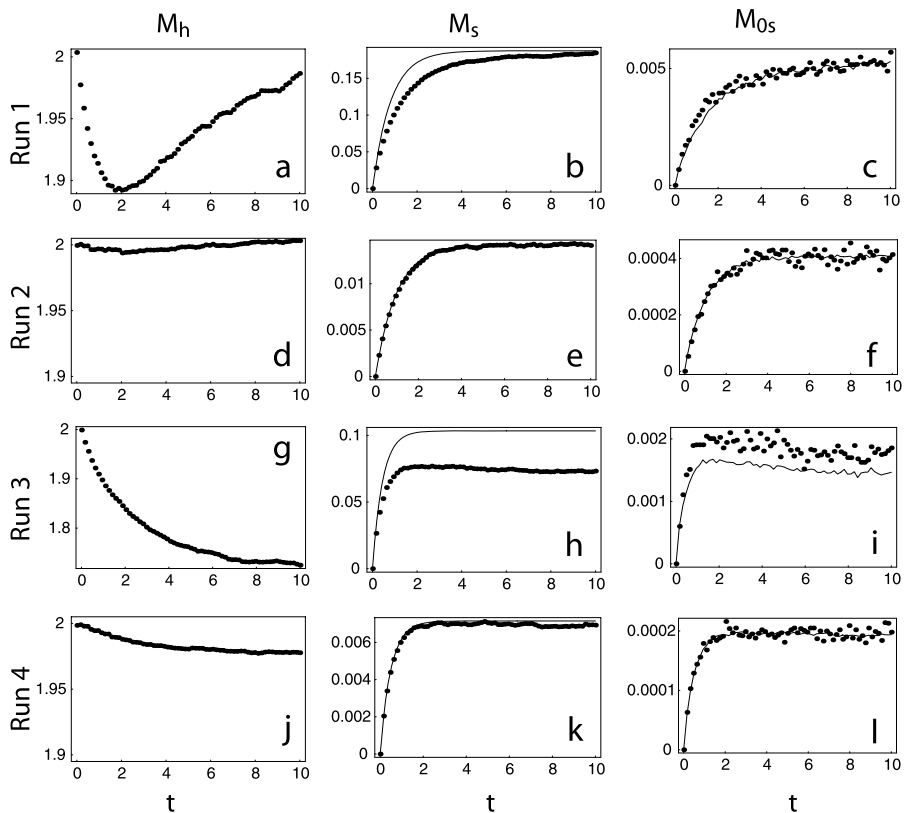


Fig. 6 Results from simulations of the spherical model. In the first two panels of each row, dots show $\langle N_h \rangle$ and $\langle N_s \rangle$ and solid curve in the middle panel shows the analytical solution for $M_s(t)$ given by (66). In the last panel, dots show $\langle N_0 N_s \rangle$ and the solid curve shows $M_{0s} = M_0 M_s$. Values of the parameters $\kappa_{0 \rightarrow s}$, $\kappa_{s \rightarrow 0}$ and $\kappa_{s \rightarrow d}$ are the same as those used to construct corresponding panels in Fig. 3.

independence $M_{0s} = M_0 M_s$. To generate this curve, the values of M_0 and M_s used are averages over the simulations.

Run 1 uses $\kappa_{0 \rightarrow s} = 1$, $\kappa_{s \rightarrow 0} = 1$ and $\kappa_{s \rightarrow d} = 0$. Results shown are averages of 1.6×10^5 simulations made over a model time of $10t'_D$. They are presented in the first row of Fig. 6. Panel (a) shows M_h decreasing by about 5% and then increasing until the end of the simulation. Panel (b) shows M_s increasing monotonically through the simulation towards the same asymptote as the $D \rightarrow \infty$ solution, but more slowly. Panel (c) shows a small discrepancy between the simulated values of M_{0s} and result predicted by statistical independence for $t < 5t'_D$.

Similar to the case of the interval model, simulations suggest that the results of the spherical model are well-approximated by the $D \rightarrow \infty$ limit when only $\kappa_{0 \rightarrow s} \ll 1$; $\kappa_{s \rightarrow 0}$ and $\kappa_{s \rightarrow d}$ may be $\mathcal{O}(1)$. Run 2 uses $\kappa_{0 \rightarrow s} = 1/16$, $\kappa_{s \rightarrow 0} = 1$ and $\kappa_{s \rightarrow d} = 0$. Results shown in the second row of Fig. 6 are averages of 6.4×10^5 simulations. In panel (d), there is a small dip in the average number of particles in the shell as they are absorbed by the empty binding site and replenished at the interface with the bulk. In panel (e), the simulations of M_s are in very good agreement with the $D \rightarrow \infty$ solution. Panel (f) shows excellent agreement between the simulation results and the predictions of statistical independence.

Run 3 uses $\kappa_{0 \rightarrow s} = 1$, $\kappa_{s \rightarrow 0} = 1$ and $\kappa_{s \rightarrow d} = 1$. Unlike the interval model, values of $M_h(t)$ and $M_s(t)$ do not decrease to 0 as t increases when $\kappa_{s \rightarrow d} > 0$. Flux from the bulk maintains the concentration in the shell. In panel (g), M_h decreases to an asymptotic value just above 1.7. M_s increases to a value that is below the $D \rightarrow \infty$ limit. This reflects the fact that the concentration in the shell is not a constant function of spatial coordinate, unlike the $D \rightarrow \infty$ limit. Panel (i) shows that $M_{0s} > M_0 M_s$.

Run 4 uses $\kappa_{0 \rightarrow s} = 1/16$, $\kappa_{s \rightarrow 0} = 1$ and $\kappa_{s \rightarrow d} = 1$. Results shown in the fourth row of Fig. 6 are averages of 2.56×10^6 simulations. In panel (j), M_h decreases to about 1.98. The concentration in the shell is slightly below its value in the bulk. As a result, in panel (k), simulated values of M_s are slightly below those given by the $D \rightarrow \infty$ limit. Panel (l) shows excellent agreement between the simulation results and the predictions of statistical independence.

3.7. Model of ATP binding to dynein

This section presents a simulation of ATP binding to dynein with a realistic set of reaction rates and demonstrates that it operates in the high D regime. The simulation is based on a fragment of the kinetic model described in the Appendix of Omoto and Johnson (1986). It considers ATP binding to a single dynein head, which is one component of a more complex mechanism. Binding of ATP to dynein induces dissociation of dynein from the microtubule complex; this complication is neglected by the model presented here.

Assume the length scale of the ATP binding site is $A = 1$ nm and that the concentration of ATP in the bulk is $C_0 = 2$ mM, which is a typical concentration of ATP in cells. The dimensionless concentration is then $c_0 = A^3 C_0 = 1.2 \times 10^{-3}$. The diffusion coefficient of ATP is $D \approx 0.15 \times 10^{-5} \text{ cm}^2 \text{ s}^{-1}$, giving a diffusion time of $t'_D = A^2/D = 6.7$ ns.

ATP associates with the microtubule-dynein complex with a first-order reaction rate of $1.5 \mu\text{M}^{-1} \text{ s}^{-1}$. Compare this with the dimensional association rate in the spherical model, which can be written

$$\lim_{n \rightarrow \infty} M_0 k_{0 \rightarrow s} / \Delta t' = D 4\pi A \kappa_{0 \rightarrow s} C(A, t'). \quad (68)$$

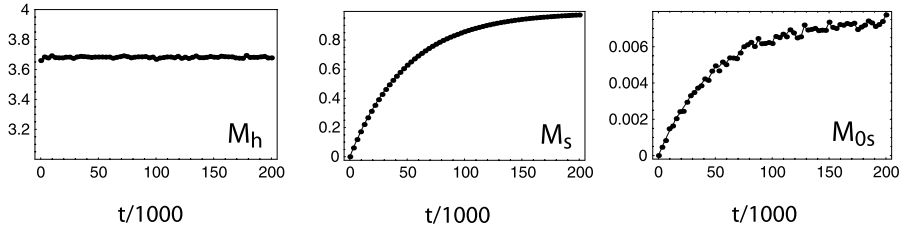


Fig. 7 Simulation of a simplified model of ATP binding to dynein. In the first two panels, dots show $\langle N_h \rangle$ and $\langle N_s \rangle$, respectively. In the middle panel, the solid curve is the solution of (66). In the last panel, dots show $\langle N_1 N_s \rangle$ and the solid curve shows $\langle N_1 \rangle \langle N_s \rangle$.

Then $D4\pi A\kappa_{0 \rightarrow s} = 1.5 \mu\text{M}^{-1} \text{s}^{-1}$, giving a value of $\kappa_{0 \rightarrow s} = 1.3 \times 10^{-3}$. ATP dissociates from the complex at a rate of 0.1 s^{-1} . Compare this with the dimensional dissociation rate in the spherical model: $k_{s \rightarrow 0} / \Delta t' = t_D^{-1} \kappa_{s \rightarrow 0}$, giving $\kappa_{s \rightarrow 0} = 6.7 \times 10^{-10}$. Finally, ATP is hydrolyzed by the dynein binding site at a rate of $k_{s \rightarrow d} / \Delta t' = 33 \text{ s}^{-1}$, giving $\kappa_{s \rightarrow d} = 2.2 \times 10^{-7}$.

The simulations use $a = 1$ and $b = 9$ and only $n = 1$ random walk site per unit length, giving $n_T = 8$. Physically, the binding site is modeled as a sphere with radius 1 nm and the shell has inner radius 1 nm and outer radius 9 nm. Results shown are averages of 2×10^5 simulations, each of which is carried out to a maximum of $t = 2 \times 10^5$. Initially, no walkers are placed in the shell. However, on the time scale of the simulations, the shell quickly equilibrates with the bulk concentration c_0 .

Results are shown in Fig. 7. In the first two panels, dots show $\langle N_h \rangle$ and $\langle N_s \rangle$ where $\langle \dots \rangle$ is an average over simulations. The solid curve in the middle panel is the solution of (66). The first panel shows that the shell occupation probability as a function of time. This is nearly constant, with a numerical value of $\langle N_h \rangle \approx 3.68$. In comparison, the theoretical value is $V_h c_0 \approx 3.66$, where V_h is the volume of the shell. The middle panel shows that the increase in the binding site occupation probability as a function of time is in excellent agreement with the $D \rightarrow \infty$ limit. In the last panel, dots show $\langle N_1 N_s \rangle$ and the curve shows $\langle N_1 \rangle \langle N_s \rangle$. The random variables N_1 and N_s are very nearly independent.

4. Summary and discussion

Two models have been presented which show how a boundary condition modeling the single-occupancy constraint can be constructed for diffusion equations from sequences of random walks. In the interval model, the diffusion equation on an interval, (2), is coupled with an equation describing the time evolution of the occupancy of the binding site, (16) through the boundary condition, (13). The system is not closed because of its dependence on the joint expectation M_{1s} . For the case of $k_{s \rightarrow d} = 0$, a simple analysis shows that, in the limit $D \rightarrow \infty$, the joint expectation can be expressed in terms of M_1 and M_s through particle number dependence, (27). For $k_{s \rightarrow d} > 0$, the same result can be obtained as an approximation. When particle number dependence holds, $M_{1s} < M_1 M_s$, occupation of sites 1 and s is anti-correlated. The anticorrelation arises from the fixed number of particles in the interval model. Further, in the limit $D \rightarrow \infty$, our analysis shows that the

interval model is described by a system of two coupled first order ODEs, (38) and (39). The limit $D \rightarrow \infty$ corresponds to infinitesimal values of $\kappa_{1 \rightarrow s}$, $\kappa_{s \rightarrow 1}$ and $\kappa_{s \rightarrow d}$. Remarkably, numerical simulations suggest that this system of two coupled ODEs approximates the solution of the interval model accurately when only $\kappa_{1 \rightarrow s} \ll 1$. The rates $\kappa_{s \rightarrow 1}$ and $\kappa_{s \rightarrow d}$ may be $\mathcal{O}(1)$.

In the spherical model, the Smoluchowski equation describing diffusion in the radial direction in a spherically symmetric system, (45), is coupled with an equation describing the time evolution of a binding site, (57), through the boundary condition (54). These last two equations depend on the joint expectation M_{0s} . A boundary condition is developed to model the interface between the shell, which is the domain of the Smoluchowski equation, and the infinite bulk outside. The boundary condition holds generally for a steady state, and not just near thermodynamic equilibrium. In the limit $D \rightarrow \infty$, sites s and 0 are statistically independent and $M_{0s} = M_0 M_s$. The number of diffusing particles is not fixed; particles can flow from the bulk into the shell. Further, in this limit, $M_s(t)$ is described by the solution of a simple linear ODE, (66). Similar to the case of the interval model, numerical simulations suggest that this limiting solution holds when only $\kappa_{0 \rightarrow s} \ll 1$. The rates $\kappa_{s \rightarrow 0}$ and $\kappa_{s \rightarrow d}$ may be $\mathcal{O}(1)$.

In order to obtain the boundary conditions for the interval and spherical models, we assumed relationships between the random walk occupation probabilities and the probability densities of the limiting diffusion processes. These approximations are given by (4) and (48). Suppose instead that the random walk occupation probabilities and the probability density of the spherical model are assumed to be related by

$$\hat{M}_i(t) = \int_{r_i^*}^{r_{i+1}^*} p(r, t) dr, \tag{69}$$

for $1 \leq i \leq n_T - 1$. For $i = 0$ integrate over (r_0, r_1^*) and for $i = n_T$ integrate over $(r_{n_T}^*, r_{n_T})$. The symbol \hat{M} is used for the occupation probabilities to avoid confusion with the assumption (48). To compare these approximations, suppose that $p(r, t)$ has a continuous second derivative with respect to r and expand $p(r, t) = T_1(r, t) + R_1(r, t)$ about $r = r_i$, where T_1 is the first order Taylor polynomial and R_1 the corresponding remainder. Integrate over the i th subinterval in Fig. 5c to obtain

$$\hat{M}_i(t) = \begin{cases} p(r_0, t) \frac{\Delta r}{2} + \frac{\partial p}{\partial r}(r_0, t) \frac{1}{8n^2} + \mathcal{O}(n^{-3}), & \text{for } i = 0, \\ p(r_i, t) \Delta r + \mathcal{O}(n^{-3}), & \text{for } 1 \leq i \leq n_T - 1, \\ p(r_{n_T}, t) \frac{\Delta r}{2} - \frac{\partial p}{\partial r}(r_{n_T}, t) \frac{1}{8n^2} + \mathcal{O}(n^{-3}), & \text{for } i = n_T. \end{cases} \tag{70}$$

Using these expressions and the expressions for the spherical model transition rates, find for $i/n \rightarrow \tilde{r} \in (1, b)$ as $i \rightarrow \infty$

$$\lim_{n \rightarrow \infty} \frac{\hat{M}_i k_{i \rightarrow i+1} - \hat{M}_{i+1} k_{i+1 \rightarrow i}}{\Delta t} = -\frac{\partial p}{\partial r}(\tilde{r}, t) + 2p(\tilde{r}, t) = j(\tilde{r}, t), \tag{71}$$

but for $i = 0$

$$\lim_{n \rightarrow \infty} \frac{\hat{M}_0 k_{0 \rightarrow 1} - \hat{M}_1 k_{1 \rightarrow 0}}{\Delta t} = -\frac{3}{4} \frac{\partial p}{\partial r}(1, t) + 2p(1, t) \neq j(1, t), \tag{72}$$

and with a result different from $j(b, t)$ for $i = n_T - 1$. Comparisons are made with the expression for the probability current j given by (47). The results of (71) and (72) are inconsistent. For example, if (54) and (57) were recalculated using the expressions for the \hat{M}_i instead of the M_i , the right-hand side of the equation corresponding to (57) would not match the right-hand side of the equation corresponding to (54) (prefixed by a minus sign and ignoring the terms corresponding to transitions into the dead state). In contrast, the corresponding expressions calculated using the M_i from (48) are consistent. Another example is given by (62) and (63). Further, the approximation given by (48) satisfies the necessary condition of detailed balance at thermodynamic equilibrium: $M_i k_{i \rightarrow j} = M_j k_{j \rightarrow i}$. For example, substitute from (48) for M_i and from (50) for $k_{i \rightarrow j}$. The balance condition is satisfied when $p(r, t) = 4\pi r^2 c_0$, corresponding to the thermodynamic equilibrium condition of constant concentration c_0 . In contrast, it can be easily seen that the assumption of (69) does not satisfy the corresponding detailed balance condition. Nevertheless, the \hat{M}_i closely approximate the M_i for n large, and therefore the arguments in this paragraph show that the results of this paper depend somewhat delicately on the approximation (48).

The spherical model is somewhat similar to the model of gated absorption studied by Doering (2000). This concerns particle concentrations outside of an “occasionally partially absorbing” sphere. For part of the time the sphere absorbs particles at a fixed rate and for the other part of the time the sphere reflects particles. The kinetics of gating are described by a two-state Markov process that is independent of the rest of the system. In this sense, fluctuations are “external.” Doering looks for “resonant activation” in this system. This phenomenon arises in some systems that involve particles crossing over fluctuating barriers. When the time scale for barrier crossing is comparable to the time scale of the fluctuations, strong correlations may arise between barrier variations and particle crossing events, increasing the flux across the barrier. However, no enhanced flux were seen in the steady state kinetics of this model of gated absorption. The author concluded that this may be due to the absence of a nonzero time scale for barrier crossing in the model.

Like this model of gated absorption, the spherical model absorbs particles at some times but not at others. However, the gating function depends on the state of the system, in particular, particles are not absorbed when the binding site is occupied. These fluctuations are “internal.” Also like the model for gated absorption, the spherical model does not have a nonzero time scale for barrier crossing. In effect, particle absorption by the empty binding site is instantaneous, although it occurs at exponentially distributed random times. Therefore, it seems unlikely that resonant activation occurs in this system. On the other hand, physical single-occupancy binding sites may well have free energy barriers that must be crossed in order that binding occurs, and these would be associated with nonzero time scales for barrier crossing.

In this paper, two diffusion processes in one spatial dimension have been obtained as the limit of a sequence of random walks. This kind of construction was also carried out in two spatial dimensions to obtain a diffusion process corresponding to a Smoluchowski equation with a diffusion matrix including off-diagonal terms (Schumaker and Watkins, 2004). In a similar manner, a diffusion in a 3D bulk coupled with diffusion on a 2D surface was constructed (Schumaker and Kentler, 1996). Constructing the diffusion process as the limit of a sequence of random walks allows one to design the behavior of the underlying trajectories. This is because the behavior of trajectories is manifest in the random walk itself and qualitative features of the behavior

are inherited in the diffusion limit. This is the idea behind a rederivation of Levitt's theory of single-ion channels (Levitt, 1986) that makes the single-ion property manifest and generalizes the single-ion boundary conditions (McGill and Schumaker, 1996; Schumaker, 2002) ("single-particle" may be a better phrase since electrical charge has no explicit role in these theories). The diffusion constructed by Schumaker and Watkins (2004) also has the single-particle property.

It appears likely that the method of constructing a diffusion as the limit of a sequence of random walks can also be used to obtain boundary conditions that describe the interaction of a bulk diffusion with a single occupancy site in other geometries. In some domain, a random walk would be constructed to converge to a diffusion process as a parameter $n \rightarrow \infty$. On the boundary of the domain, the random walks would be constructed to give certain desired behaviors. For example, random walk sites along one portion of the boundary could all link to a single-occupancy site. The appropriate scaling of the transition rate from the single occupancy site into the domain with n could be determined by requiring that transitions were exponentially distributed in time. Physically, this distribution corresponds to escape over a free energy barrier (see the discussion below (8)). Scaling of the transition rate from the domain back to the single occupancy site with n would then be determined by the requirement that detailed balance is satisfied.

On portions of the domain that modeled an interface with diffusion in a infinite bath, new particles can be introduced with exponentially distributed waiting times; see the derivation of (58) and the associated discussion. According to the result of Nadler et al. (2001), this is the correct model for the arrival of independent, identical diffusers. The rate of escape from the domain of the random walk into the bath would then be determined by detailed balance. However, this approach ignores particles that escape from the bath and then return (Nadler et al., 2003). Yet, when applied in the spherical model, it yields a boundary condition that is satisfied by the general steady state solution for particle flux. This result can be explained in the following way. The spherical model has only 1 spatial dimension, the radial variable r . In this setting, a particle that escapes from the shell into the bulk and then returns follows a closed path. At any spatial point, the steady state flux of such particles in the direction of increasing r must equal the steady flux in the opposite direction. Therefore, they contribute no net flux and, by Fick's law, make no contribution to $c'_{SS}(r)$, where c_{SS} is the steady state concentration. The integration constant is determined by the boundary condition, $c_{SS}(r) \rightarrow c_0$ as $r \rightarrow \infty$, and, therefore, reentering particle make no contribution to c_{SS} . It would be very interesting to know whether this result generalizes to a larger class of particle flow fields (for example, irrotational flows).

Acknowledgements

The author is very grateful to Charlotte Omoto for discussions concerning the model of ATP binding to dynein and to David Kramer for introducing him to the light reactions of photosynthesis. He thanks David Watkins for his careful reading of an early draft of this manuscript. Finally, he appreciates the detailed and constructive comments made by two anonymous referees.

References

- Agmon, N., Hopfield, J.J., 1983. Transient kinetics of chemical reactions with bounded diffusion perpendicular to the reaction coordinate: intramolecular processes with slow conformational changes. *J. Chem. Phys.* 78(11), 6947–6959.
- Bernèche, S., Roux, B., 2003. A microscopic view of conduction through the *Streptomyces lividans* K^+ channel. *Proc. Natl. Acad. Sci. USA* 100, 8644–8648.
- Doering, C.R., 2000. Effect of boundary condition fluctuations on Smoluchowski reaction rates. In: Freund, J.A., Pöstel, T. (Eds.), *Stochastic Processes in Physics Chemistry and Biology*, pp. 316–326. Springer, Berlin.
- Elston, T.C., Doering, C.R., 1996. Numerical and analytical studies of nonequilibrium fluctuation-induced transport processes. *J. Stat. Phys.* 83, 359–383.
- Gardiner, C.W., 1983. *Handbook of Stochastic Methods*. Springer, Berlin.
- Gillespie, D.T., 1977. Exact stochastic simulations of coupled chemical reactions. *J. Phys. Chem.* 81, 2340–2361.
- Im, W., Seefeld, S., Roux, B., 2000. A Grand Canonical Monte Carlo Brownian dynamics algorithm for simulating ion channels. *Biophys. J.* 79, 788–801.
- Kirchhoff, H., Horstmann, S., Weis, E., 2000. Control of photosynthetic electron transport by PQ diffusion microdomains in thylakoids of higher plants. *Biochim. Biophys. Acta* 1459, 148–168.
- Kramers, H.A., 1940. Brownian motion in a field of force. *Physica* 7, 284–304.
- Levitt, D.G., 1986. Interpretation of biological ion channel flux data: reaction rate versus continuum theory. *Annu. Rev. Biophys. Biophys. Chem.* 15, 29–57.
- Liggett, T.M., 1985. *Interacting Particle Systems*. Springer, New York.
- Lin, J.-C., Doering, C.R., ben-Avraham, D., 1990. Joint density closure schemes for a diffusion-limited reaction. *Chem. Phys.* 146, 355–371.
- McGill, P., Schumaker, M.F., 1996. Boundary conditions for single-ion diffusion. *Biophys. J.* 71, 1723–1742.
- Nadler, B., Naeh, T., Schuss, Z., 2001. The stationary arrival process of independent diffusers from a continuum to an absorbing boundary is Poissonian. *SIAM J. Appl. Math.* 62(2), 433–447.
- Nadler, B., Naeh, T., Schuss, Z., 2003. Connecting a discrete ionic simulation to a continuum. *SIAM J. Appl. Math.* 63(3), 850–873.
- Omoto, C.K., Johnson, K.A., 1986. Activation of the dynein adenosinetriphosphatase by microtubules. *Biochemistry* 25, 419–427.
- Perko, L., 2001. *Differential Equations and Dynamical Systems*, 3rd edn., p. 245. Springer, Berlin.
- Risken, H., 1989. *The Fokker–Planck Equation*. Springer, Berlin.
- Schumaker, M.F., 2002. Boundary conditions and trajectories of diffusion processes. *J. Chem. Phys.* 116(6), 2469–2473.
- Schumaker, M.F., Kentler, C.J., 1996. Far field analysis of coupled bulk and boundary layer diffusion toward an ion channel entrance. *Biophys. J.* 74, 2235–2248.
- Schumaker, M.F., Watkins, D.S., 2004. A framework model based on the Smoluchowski equation in two reaction coordinates. *J. Chem. Phys.* 121, 6134–6144.
- Song, Y., Zhang, Y., Shen, T., Bajaj, C.G., McCammon, J.A., Baker, N.A., 2004. Finite element solution of the steady-state Smoluchowski equation for rate constant calculations. *Biophys. J.* 86, 2017–2029.
- Wang, H., Peskin, C.S., Elston, T.C., 2003. A robust numerical algorithm for studying biomolecular transport processes. *J. Theor. Biol.* 221, 491–511.
- Xing, J., Wang, H., Oster, G., 2005. From continuum Fokker–Planck models to discrete kinetic models. *Biophys. J.* 89, 1551–1563.